Odd Stator Slot Numbers in Brushless DC Machines—An Aid to Cogging Torque Reduction

David G. Dorrell[1] and Mircea Popescu[2]

[1]University of Technology Sydney, Sydney NSW 2007, Australia
[2]Motor Design Ltd, Ellesmere, Shropshire SY12 0EG, U.K.

Brushless permanent-magnet dc machines often use an integral number of slots per pole (e.g., 3 slots/pole) with fully pitched coils in order to obtain a good trapezoidal back-electromotive-force (emf) waveform. However, this can lead to high cogging torque and load torque ripple. A simple solution is to add one additional slot so that the reluctance slotting that causes the ripple is removed, but the winding pattern is closely retained. This paper illustrates that simple design modification, where one additional slot is used so that the machine does not have an integral number of slots per pole. In this paper, the arrangement is analyzed using simple winding analysis and a finite-element analysis which gives more preciseness to calculations. It is found that there is a substantial reduction in cogging and load torque oscillation, thus proving the principle. However, the stator windings are slightly unbalanced and this can lead to vibration. This is also investigated and the resulting unbalanced magnetic pull under load is found to be present but of a low magnitude.

Index Terms—**Brushless permanent magnet DC motor, cogging torque, unbalanced magnetic pull (UMP), windings.**

I. Introduction

BRUSHLESS DC machines (BDCMs) often use full-pitched coils with integer slots/pole in order to obtain trapezoidal back-electromotive-force (emf) waveforms. The rotor is usually a surface magnet structure. This can produce high cogging torque during unexcited rotation and torque ripple when excited. A variation of this is the type of machine studied here. These machines are popular for high-efficiency power-drive motors and utilize the ferrite of rare-earth magnets.

There are many options for reducing the torque ripple, including skewing, tooth bifurcation, and careful slot opening design. There are also many alternatives and more novel designs although the slotted radial-flux arrangement still represents the main solution. A variation of using the "odd slot" method was put forward in [1] where the use of an odd number of slots per pole was investigated. Reference [2] assessed the use of preferred slot combination but all of the slot numbers used were even numbers. The use slot shaping and geometry was studied in [3] although the best results appeared for fractional slot machines.

If a surface magnet rotor is used, then it is possible to move the magnets slightly to reduce cogging effects. This has been investigated by several researchers and in [4], this technique is illustrated. However, care has to be taken to position the short-pitched magnets. Notches in stator teeth (additional surface slots in the stator tooth) also help minimize the cogging torque. A review of cogging torque reduction, which focuses on notches in stator teeth, was carried out in [5]. Bifurcated stator teeth were also used in [6]; however, the focus in this study was the use of incomplete magnetization of the magnets. This appears to be difficult to control in-series manufacturing but it is an interesting study.

The authors were unable to find any study in the literature which implemented the concept put forward here, where there is an addition of one slot to the stator in an integral number of slots per pole machine, to give an odd number of slots on the stator. This will reduce the cogging and load ripple but may produce unbalanced magnetic pull (UMP). Studies in [7] and [8] gave an indication of the levels of UMP that can occur in brushless fractional-slot ac machines. UMP is also assessed here, which is helpful in assessing possible bearing wear. The authors were surprised that a straightforward design idea appears not to have been reported; therefore, they believe this paper will be a useful addition to the body of work on BDCM design and will be of great interest to manufacturers since it represents very little change in manufacturing technique. Indeed, it may simplify and reduce manufacturing cost since skewing can be expensive. In addition, skewing can reduce the trapezoidal nature of back-emf so while cogging (which is a reluctance torque) is reduced by skewing, excitation torque ripple (which can be either cogging effects or excitation torque effects) increases.

II. Theory

A. Design Modification

The concept put forward in this paper is that in a BDCM, where fully pitched coils and integral slots per pole are required to produce a good trapezoidal back-emf waveform, one additional slot can be used in order to produce a fractional slot arrangement. This will reduce slotting effects which generate cogging torque on no load and torque ripple onload. This is a reluctance torque effect and it is well known that fractional slot arrangements are much less susceptible to reluctance torques due to the reduction in reluctance variation between tooth and magnet alignment/nonalignment. The equation for the slot number is quite straightforward. For a N-phase machine with P_m poles (and p_m pole pairs), then the number of slots S is

$$S = N \times P_m + 1. \tag{1}$$

In this paper, a three-phase, eight-pole motor is investigated. An integral slot/pole machine with 24 stator slots is compared to a 25-slot stator configuration. Both machines are analyzed in order to enable a complete assessment of the performance. In the next section, a simple winding analysis is put forward in order to investigate the winding unbalance.

B. Winding Harmonic Analysis

The winding is slightly unbalanced so the winding analysis has to be addressed. Brushless ac motors strive to obtain a sinusoidal back-emf, and the machine is fed with a balanced three-phase current set whereas a dc machine uses a trapezoidal current wave where

$$i_W(t) = \mathrm{Re}\left[\sum_{m=1}^{\infty} \frac{\overline{I}_s}{m} e^{jm\left[\omega t + a^{(1-W)}\right]}\right]_{m=1,-5,7,-11,\ldots} \quad (2)$$

where W is the phase number and using the identity $a = \exp(j2\pi/3)$ and k is the inverse of the rotor radius. If the three-phase supply is balanced with series-connected stator windings, the MMF wave is

$$j_{st}(y,t) = \mathrm{Re} \sum_{n=-\infty}^{\infty} \sum_{m=1}^{\infty} \overline{J}_{st}^{n,m} e^{j(m\omega t - np_m ky)} \quad (3)$$

where for a balanced three-phase current set, the MMF (or surface current density) can be denoted as

$$\overline{J}_{st}^{n,m} = \overline{N}_{st}^{n}\left(1 + a^{(n-m)} + a^{(m-n)}\right)\frac{\overline{I}_s}{m}. \quad (4)$$

The stator winding coefficient of one phase winding is

$$\overline{N}_{st}^{n} = \frac{k}{2\pi}\sum_{w=1}^{N_w} k_s C_w e^{jnp_m k y_w} \quad (5)$$

where N_w is the number of slots that the winding is located in, C_w is the number of series winding turns in a slot, and y_w is the linear spatial location of the slot around the stator surface from a reference angular zero point so that $ky = \theta$. The slot opening factor is defined by the slot opening b_s (in meters) so that

$$k_s = \frac{2\sin(0.5np_m k b_s)}{np_m k b_s}. \quad (6)$$

Ampere's circuital law can be applied, which leads to a distribution for the air-gap flux density due to the stator magnetomotive forces (MMF) waves. This is described in detail in [9]. However, for a balanced three-phase winding, there will be spatial winding harmonics that correspond to $n = 1, -5, 7$, etc. (i.e., there are no third harmonics and there is no backwards rotating fundamental flux wave). However, in the winding used in the odd slot machine, there is an unbalanced winding so that (4) has to be modified to

$$\overline{J}_{st}^{n,m} = \left(\overline{N}_{st}^{n1} + \overline{N}_{st}^{n2} a^{-m} + \overline{N}_{st}^{n3} a^{m}\right)\frac{\overline{I}_s}{m} \quad (7)$$

where 1, 2, and 3 are the phase numbers. There will backwards and forwards components of each spatial harmonic. We can define the backwards and forwards winding coefficients as

$$\overline{N}_{st}^{nF} = \frac{\left(\overline{N}_{st}^{n1} + \overline{N}_{st}^{n2} a^{-n} + \overline{N}_{st}^{n3} a^{n}\right)}{3}$$
$$\overline{N}_{st}^{nB} = \frac{\left(\overline{N}_{st}^{n1} + \overline{N}_{st}^{n2} a^{n} + \overline{N}_{st}^{n3} a^{-n}\right)}{3} \quad (8)$$

where nF is when $n > 0$ and nB is when $n < 0$. Higher winding harmonics generate some torque ripple and, for a fully pitched winding, will be low. The unbalance will be for the main winding harmonic and this is what will be studied. The analysis is performed using finite-element analysis to that the calculation of the forwards and backwards winding harmonics are purely for indicative purposes. The windings for the 24- and 25-slot machine are investigated in the following sections.

TABLE I
MOTOR PARAMETERS

Motor Parameter	Value
Common Rotor	
Diameter	50 mm
Pole number	8
Rotor weight	0.9 Kg
Axial length	50 mm
Magnet thickness	5.5 mm
Magnet pitch	170 elec deg
Magnet material	NdFeB, B_r = 1.12 T
Air-gap length	1 mm
24 and 25 Slot Stator	
Tooth width	3 mm
Slot opening	2 mm
Slot depth	14 mm
Common winding	
Series connected coils/phase	8
Series turns per coil	12
Turn diameter	1 mm
Pitch of coils	See Fig. 1 for layout

C. Machine Specification

A machine specification is required to carry out the simulations. As previously mentioned, an eight-pole motor was chosen with either 24 slots or 25 slots depending on whether the machine had the additional slot.

The number of coils is identical so the decision has been made to use exactly the same turn number and wire diameter. The tooth width was kept constant; while it could be adjusted to maintain the same flux levels, it does not make very much difference. Therefore, the 25-slot machine has a slightly higher slot fill factor. A specification is given in Table I for each machine while the winding layouts are illustrated in Fig. 1. This is a relatively small machine. The rotor weight is only 0.9 kg. When the current peak is 15 A, the current density is 15.6 A/mm^2. This is a high value; good cooling would be required.

D. Winding Harmonic Calculations

For the windings in Fig. 1, the forward and backward winding harmonics can be calculated. In Table II, only the main winding (eight-pole) wind harmonics are included for clarity. The winding coefficients in (8) are also normalized by division by $2kT_{ph}/(2\pi)$, where T_{ph} is the total number of series-connected phase turns and k_s is taken as 1. It can be seen that the backward winding harmonic is small even for the 25-slot stator. As expected, for the 24-slot fully pitched winding, the winding coefficient is unity due to the normalization.

III. Simulations

A. Open-Circuit Voltages

The machines were modeled in *SPEED* PC-BDC (from the University of Glasgow, U.K.) and passed through to *SPEED* PC-FEA in order to run finite-element analysis. These were static 2-D solutions, and the rotor was stepped round to obtain flux linkages. From these, open-circuit voltages were obtained. The simulations were conducted at 1000 r/min. Fig. 2 shows the voltage waveforms. It can be seen that the 25-slot voltages appear virtually balanced and of a similar magnitude to the 24-slot

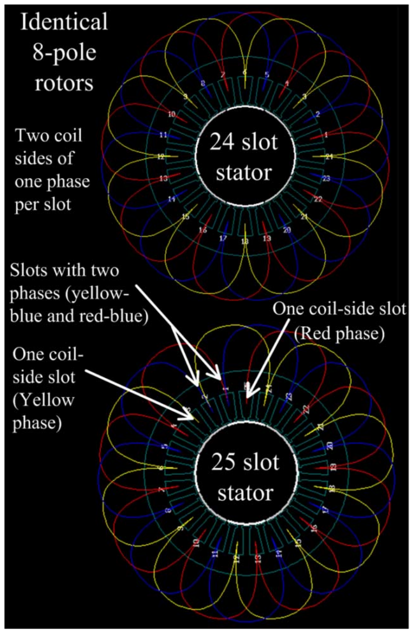

Fig. 1. The 24- and 25-slot three-phase windings.

TABLE II
FUNDAMENTAL WINDING HARMONICS (NORMALIZED)

Normalized winding coefficients	$\bar{N}_{st}^{nF}$	$\bar{N}_{st}^{1B}$
25 slot stator	0.9566	0.023
24 slot stator	1	0

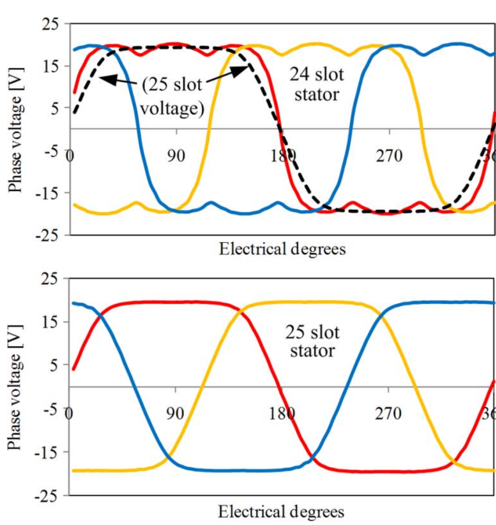

Fig. 2. The 24- (top) and 25- (bottom) slot stator machine open-circuit voltage at 1000 r/min. The 25-slot red phase is shown in the top graph for comparison.

stator machine. The waveform is almost trapezoidal which may lead to some excitation torque ripple under dc control. This machine has no skew since the additional slot aims at reducing the cogging as an alternative to skew.

B. Load Operation

The machine was simulated by using current/flux-linkage loops—i-Psi loops (where the rotor and current vector are stepped round together in the finite-element analysis and the area enclosed in the loop represents the energy conversion for one electric cycle; these are commonly used for switched reluctance machine torque calculation). This method gives an accurate value for the average electromagnetic torque. The instantaneous torque was also calculated and these are shown in Fig. 3. As expected, the 24-slot stator gives substantial cogging torque on no load and when loaded. The load current is trapezoidal as illustrated. It can be seen that this torque ripple is not present to the same extent for the 25-stator slot machine. The high-frequency torque ripple is the cogging torque because there is now a fractional slot arrangement. Since the back-emf is not as trapezoidal as the 24-slot stator arrangement, then there is some 6th harmonic torque ripple. There is still some slight torque ripple with the 25-slot stator. Some skew can be introduced to eliminate this but the required skew will be much less than that required for the 24-slot machine since the torque ripple frequency is much higher.

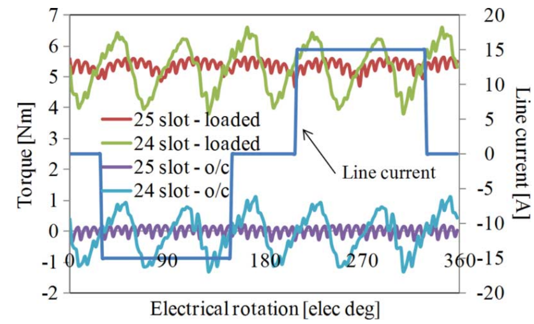

Fig. 3. The 24- and 25-slot stator machine—open-circuit cogging torque and load torque (the load current is 15 A peak and shown).

C. Mean Torque and Torque Reduction Due to Skew

The mean torque for the 24- and 25-slot stators is about the same—the 24-slot stator gives 5.38 Nm and the 25-slot stator gives 5.32 Nm (obtained from I-Psi loops). Skewing the rotor in the 24-slot machine will produce a nontrapezoidal voltage waveform and reduce the linkage so that the torque is reduced. It was found that the mean toque was 4.97 Nm with excitation torque ripple—this is a 6.5% reduction. This shows that the addition of an odd slot produces better performance than skewing the rotor or stator.

D. UMP Consideration

The UMP at open circuit and under full load is shown in Fig. 4. This is obtained from the finite-element analysis and two stress integrals are taken around the air gap (at different radii) and the mean is taken. Three-hundred sixty points (N_{points}) are used around the integral, and the normal force on the rotor surface is vectorized into horizontal and radial directions

$$F_{\text{net}} = |F_x + jF_y| = \left| \sum_{n=1}^{N_{points}} \left[\left(\frac{2\pi R}{N_{points}} \right) \frac{B_{\text{radial}}^2(y)}{2\mu_0} \times \{\cos(ky_n) + j\sin(ky_n)\} \right] \right| \quad (9)$$

where R is the radius of the air-gap stress integral, $ky_n = \theta_n =$ is the angular position of the point around the air gap, and x and y are the orthogonal radial directions. Mean peak UMP at full load is about three times the force due to the weight of the

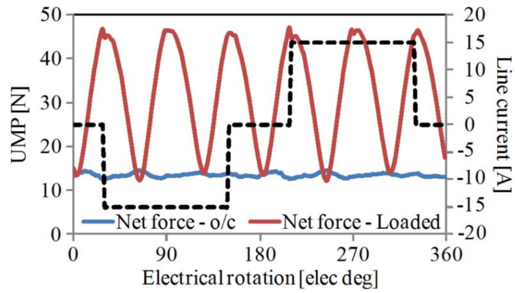

Fig. 4. UMP in a 25-slot stator machine when the machine is open circuit and fully loaded—radial force magnitude (which will vary in direction). The current waveform for phase 1 is given for reference.

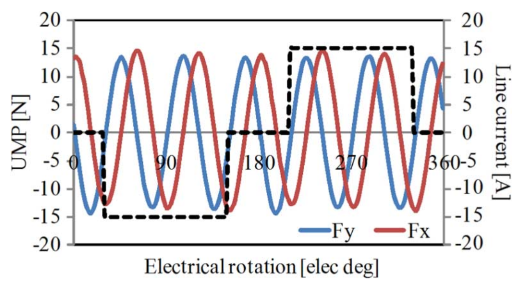

Fig. 5. UMP in the 25-slot stator machine when open circuit with the force broken down into Fx and Fy—this shows a rotating force vector.

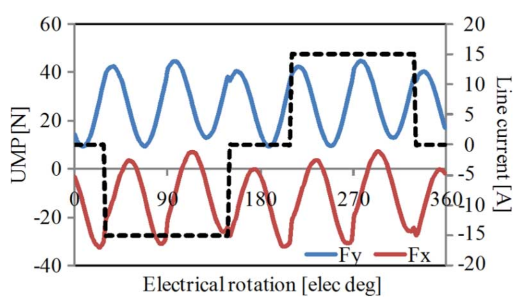

Fig. 6. UMP in the 25-slot stator machine when fully loaded with the force broken down into Fx and Fy—this shows a rotating force vector and a constant pull.

rotor. There is torque due to the stator slot asymmetry (hence, UMP on the open circuit) which is a rotating force vector as can be observed in Fig. 5. When the machine is fully loaded, there is a constant force or radial pull toward the slots with only one coil side illustrated in Fig. 6 (in Fig. 1, F_x is upwards in the vertical direction and F_y is horizontal and to the left). There is also the slot asymmetry UMP, which is a rotating force vector and generates the vibrating UMP components.

The UMP, due to the use of the 25-slot stator, appears to give higher radial forces compared to the rotor weight which may cause bearing wear; this was purposely done. However, this is because the motor is quite small. If we scale the machine, we find that for rotor length L and diameter D

$$\text{Rotor weight and torque} \propto LD^2$$
$$\text{Unbalanced magnetic pull} \propto LD.$$

Obviously, the weight is a volumetric quantity but the torque is a function of the product of the stress on the surface (proportional to D) and torque arm length $(D/2)$ whereas the UMP is simply a function of the stress. If we triple the axial length and diameter of the machine to turn it into a large motor, where bearing wear will be more important, then the weight increases by 27 times but the UMP will increase by 9 times. The UMP, due to the odd slot, will then be about $9 \times 45 = 405$ N, whereas the radial force due to the rotor weight will be $9.81 \times 0.9 \times 27 = 238$ N. If the diameter and axial length increase by nine times (which would be a very large PM motor), the UMP would be 3645 N and the rotor weight force would be 6436 N. This is only a basic sizing calculation, but it shows that the additional wear due to the UMP is most relevant in small machines and decreases with increasing size. In large machines, the odd-slot UMP will be negligible compared to the weight of the rotor that the bearings have to support.

IV. Conclusion

This paper has illustrated that one additional slot can be used to eliminate cogging and load torque ripple in an integral slot/pole dc motor aimed at high-efficiency power drives. It gives better results compared to skewing for the investigated motor design. While the UMP seems relatively high, the sample machine is very small. It is shown that in larger machines, this should not be a problem. For reference, various small ac fractional slot machines actually have much higher UMP due to asymmetry in the windings [8] and operate successfully. One additional slot leads to two half empty slots in the machine which are nearly one-pole pitch apart. These need to be packed in the manufacturing process, or could be used for an additional search coil for rotor positioning.

References

[1] S.-H. Han, T. M. Jahns, W. L. Soong, M. K. Guven, and M. S. Illindala, "Torque ripple reduction in interior permanent magnet synchronous machines using stators with odd number of slots per pole pair," *IEEE Trans. Energy Convers.*, vol. 25, no. 1, pp. 118–127, Mar. 2010.

[2] A. J. Mitcham, G. Antonopoulos, and J. J. A. Cullen, "Favourable slot and pole number combinations for fault-tolerant PM machines," *Proc. Inst. Elect. Eng., Elect. Power Appl.*, vol. 151, no. 5, pp. 520, 525, 2004.

[3] Y. Yang, X. Wang, R. Zhang, C. Zhu, and T. Ding, "Research of cogging torque reduction by different slot width pairing permanent magnet motors," in *Proc. Int. Conf. Elect. Mach. Syst.*, 2005, vol. 1, pp. 367–370.

[4] M. S. Islam, S. Mir, and T. Sebastian, "Issues in reducing the cogging torque of mass-produced permanent magnet brushless DC motor," in *Proc. IEEE 38th Annu. Ind. Appl. Conf.*, 2003, vol. 1, pp. 393–400.

[5] S. Murthy, B. Derouane, B. Liu, and T. Sebastian, "Minimization of torque pulsations in a trapezoidal back-EMF permanent magnet brushless DC motor," in *Proc. IEEE 34th Annu. Ind. Appl. Conf.*, 1999, vol. 2, pp. 1237–1242.

[6] C. S. Koh and J.-S. Seol, "New cogging-torque reduction method for brushless permanent-magnet motors," *IEEE Trans. Magn.*, vol. 39, no. 6, pp. 3503–3506, Nov. 2003.

[7] D. G. Dorrell, M. Popescu, and D. Ionel, "Unbalanced magnetic pull due to asymmetry and low-level static rotor eccentricity in fractional-slot brushless permanent-magnet motors with surface-magnet and consequent-pole rotors," *IEEE Trans. Magn.*, vol. 46, no. 7, pp. 2675–2685, Jul. 2010.

[8] Z. Q. Zhu, D. Ishak, D. Howe, and J. Chen, "Unbalanced magnetic forces in permanent-magnet brushless machines with diametrically asymmetric phase windings," *IEEE Trans. Ind. Appl.*, vol. 43, no. 6, pp. 1544–1553, Nov./Dec. 2007.

[9] D. G. Dorrell, "Sources and characteristics of unbalanced magnetic pull in three-phase cage induction motors with axial-varying rotor eccentricity," *IEEE Trans. Ind. Appl.*, vol. 47, no. 1, pp. 12–24, Jan./Feb. 2011.